Desert Ecosystem Engineering Journal (2026) 15 (2), page 1-17

Assessment of Climate Variables under CMIP6 Future Climate Scenarios in a Semi-Arid Region of Northwestern Iran

Raoof Mostafazadeh[1*], Ali Nasiri Khiavi[2], Shahnaz Mirzaei[3]

Received: 2026/04/30 Accepted: 2026/06/27

Abstract

Climate change, largely driven by anthropogenic activities, has intensified the frequency and severity of extreme weather events, including floods, droughts, hailstorms, heatwaves, and anomalous cold spells. This study evaluates the performance of three CMIP6 models (ACCESS-CM2, MIROC6, and NESM3) in simulating daily precipitation and temperature for the flood-prone Gharesou watershed in Ardabil, Iran. The models were validated against observed data from 1984–2014 using statistical metrics, including Root Mean Square Error (RMSE), Percent Bias (PBIAS), and the Nash-Sutcliffe Efficiency (NSE). Following validation, future projections were downscaled and bias-corrected under SSP1-2.6, SSP2-4.5, and SSP3-7.0 scenarios using the delta change method. Based on the superior performance in PBIAS and NSE metrics across all stations—with minor exceptions in specific precipitation and maximum temperature parameters at the Ardabil and Namin stations—the ACCESS-CM2 model was selected for long-term projections. The results indicate a general downward trend in monthly precipitation, with localized exceptions during the June–August period in Ardabil, March–August at the Airport station, and July in Namin and Nir. A comparative analysis between observed and projected mean annual precipitation under the SSP1-2.6 scenario reveals site-specific variations: declines of 31.07 mm, 37.60 mm, and 116.69 mm at the Ardabil, Namin, and Nir stations, respectively, alongside a marginal increase of 1.44 mm at the Ardabil airport station. Furthermore, all scenarios project a consistent rise in mean annual maximum and minimum temperatures. Specifically, the projected increase in maximum temperature ranges from 1.2 °C (SSP2-4.5, Ardabil) to 2.05 °C (SSP1-2.6, Namin), while minimum temperatures are expected to rise by 3.65 °C (SSP2-4.5, Namin) to 7.75 °C (SSP1-2.6, Ardabil airport). These forecasts, characterized by decreasing precipitation and significant warming, underscore the likelihood of imminent climate-driven extremes. Consequently, these findings provide a critical foundation for water resource managers to develop targeted risk mitigation strategies and enhance environmental and hydrological resilience in the region.

Keywords: Delta change factor, Bias correction, ACCESS-CM2 model, SSP1-2.6 scenario, Gharesou watershed

1. Department of Natural Resources, Faculty of Agriculture and Natural Resources, Member of Water Management Research Center, University of Mohaghegh Ardabili, Ardabil, Iran.
* Corresponding Author. raoofmostafazadeh@uma.ac.ir
2. Ardabil Agricultural and Natural Resources Research and Education Center, Agricultural Research, Education and Extension Organization (AREEO), Ardabil, Iran, a.nasiri@areeo.ac.ir
3. Department of Watershed Management, Faculty of Range and Watershed Management, Gorgan University of Agricultural Sciences and Natural Resources, Gorgan, Iran, mirzaeishahnaz@gmail.com

DOI: 10.22052/deej.2026.258580.1140

1. Introduction

1.1. Background

Climate is defined by the long-term averages of weather conditions in a given region, and the shifting of these patterns represents a fundamental challenge in contemporary environmental science (Luo & Yu, 2012). Climate change manifests at both local and global scales through gradual alterations in climatic components, such as temperature, humidity, cloud cover, wind, and precipitation (Wang et al., 2023). Since the Industrial Revolution, anthropogenic greenhouse gas emissions, particularly carbon dioxide, have driven a marked increase in global mean temperatures (IPCC, 2013). This warming trend is inextricably linked to shifts in precipitation patterns; as warmer air exhibits an increased water vapor saturation point and enhanced moisture-holding capacity, the atmosphere becomes more conducive to frequent and severe hydro-climatic extremes (Dannenberg et al., 2019; Alimohamadian et al., 2026). This interdependence between climatic variables complicates the accurate prediction of their spatiotemporal dynamics (Meresa et al., 2022). Furthermore, as precipitation and temperature serve as primary inputs for natural ecosystems, any deviation in these variables exerts a direct influence on ecosystem structure and productivity (Su et al., 2016). Consequently, robust climate projections are essential for informed decision-making in hydrology, agriculture, natural hazard assessment, and water resource management (Asgari et al., 2025). The reliability of these managerial decisions hinges upon the quality, consistency, and completeness of the underlying climatic datasets (Liu et al., 2021).

Over the past few decades, international collaborative efforts led by the Intergovernmental Panel on Climate Change (IPCC) have utilized Global Climate Models (GCMs) to generate comprehensive projections of past and future climatic conditions (Stocker et al., 2013). These models simulate complex interactions between the atmosphere, oceans, cryosphere, and land surface, providing a systematic framework for understanding how climatic variables evolve over time (Su et al., 2016). The Coupled Model Intercomparison Project (CMIP) serves as the primary repository for these simulations. The sixth phase of this project (CMIP6), established to refine climate projections, incorporates enhanced physical process simulations and improved dynamic characteristics compared to its predecessor, CMIP5, resulting in a significant reduction of biases in key variables such as temperature and precipitation (Eyring et al., 2016; Döscher et al., 2021). These data, whether used directly or following regional downscaling, form the scientific basis for assessing climate change impacts at local and regional scales (Voldoire et al., 2019).

Climate projections in the Sixth Assessment Report are based on the Shared Socioeconomic Pathways (SSPs), which integrate climate change projections with diverse socioeconomic trajectories—including global population growth, economic development, and technological advancement—to analyze feedback mechanisms (Rogelj et al., 2018; Estoque et al., 2020). The primary SSP scenarios encompass: (1) SSP1 (Sustainability), characterized by sustainable development, reduced resource consumption, and environmental consciousness; (2) SSP2 (Middle-of-the-road), representing a continuation of historical socioeconomic trends; (3) SSP3 (Regional rivalry), marked by geopolitical conflict, high population growth in developing nations, and significant environmental degradation; (4) SSP4 (Inequality), defined by uneven technological progress and high social conflict; and (5) SSP5 (Fossil-fueled development), which emphasizes rapid economic growth coupled with a continued reliance on fossil fuels.

1.2. Literature review

Numerous studies have investigated the multifaceted impacts of climate change on various sectors, with a particular focus on hydrological hazards such as floods and droughts. Internationally, Meresa et al. (2022) examined the influence of climate change on extreme precipitation and peak discharges in Ethiopia’s Awash Basin. By employing bias-correction techniques—specifically Statistical Quantile Factor (SQF), Distribution Quantile Mapping (DQM), and Empirical Quantile Mapping (EQM)—they demonstrated that projected increases in precipitation intensity would significantly elevate future flood magnitudes. Similarly, Coelho et al. (2022) utilized the Partial Duration Series (PDS) method with CMIP6 outputs (CESM2-LE model) to assess extreme precipitation in the Contiguous United States (CONUS), forecasting an intensification of 10%–80% by 2100. In China, Wang et al. (2023) and Wu et al. (2023) analyzed the Changtan and Songhua River Basins, respectively. Their findings highlighted consistent upward trends in precipitation intensity and associated flood risks, despite the inherent uncertainties in high-resolution projections. Furthermore, Wang et al. (2024) investigated the Shiyang River Basin, demonstrating that climate change significantly alters seasonal precipitation distribution and runoff sensitivity across varying SSP scenarios.

Domestically, research in Iran has increasingly leveraged CMIP6 datasets to assess regional climate shifts. Zarrin and Dadashi-Roudbari (2021) evaluated global climate models across diverse Iranian climatic zones, noting that precipitation sensitivity is highest in arid regions. Focusing on station-specific impacts, Iranshahi et al. (2023) utilized Feed-Forward Neural Networks (FFNN) and the Firefly Algorithm (FFA) to project temperature and precipitation trends in the Aleshtar and Khorramabad stations, reporting a clear pattern of rising temperatures and declining precipitation. Zareian et al. (2023) and Ansari et al. (2022) conducted comprehensive evaluations of model performance, emphasizing that the accuracy of CMIP6 models is highly dependent on local climatic characteristics. More recently, Khansalari and Mohammadi (2024) applied a weighted multi-model ensemble to evaluate extreme precipitation indices across Iran, concluding that climate change will likely intensify hydrological hazards, particularly under high-emission scenarios.

Synthesizing these findings, it is evident that climate change is fundamentally altering precipitation and temperature regimes, thereby heightening the risk of extreme hydrological events. While studies consistently report increased warming and shifts in precipitation patterns, the precision of these projections remains contingent upon the application of robust bias-correction and downscaling techniques. Despite the growing body of literature, there remains a notable dearth of research specifically focusing on the Gharesou watershed in Ardabil Province. Given the regional sensitivity to hydro-climatic variability, this study aims to address this research gap by utilizing bias-corrected daily CMIP6 projections to assess future changes in precipitation and temperature, providing critical data for local risk management and environmental planning.

1.3. Scope and objective

The investigation of climate change impacts on water resources, agriculture, and natural hazards—particularly floods and droughts—has become a priority in environmental research (Wu et al., 2023; Mostafazadeh et al., 2025). Escalating global temperatures and the increased frequency of high-intensity precipitation events have significantly heightened the risk of climate-induced disasters (Ouyang et al., 2015). Consequently, effective management strategies must prioritize hazard mitigation, vulnerability reduction, and the long-term sustainability of land and water resources. Central to these objectives is the precise assessment of precipitation and temperature, as these variables serve as the primary drivers of hydrological processes and environmental change.

The Gharesou watershed represents one of the most critical hydrological systems in northwestern Iran. Extending from the high-altitude regions of Mount Sabalan to the

Ardabil Plain, the basin exhibits significant climatic and topographic diversity (Hazbavi et al., 2025). As the primary source of water for agricultural, environmental, and socio-economic activities in Ardabil Province, the Gharesou River—with an average annual discharge of approximately 554 million m³—is vital for regional water supply and flood regulation. Furthermore, the watershed serves as the lifeblood of the Ardabil Plain, a key agricultural hub in the region. Given the potential for climate-induced shifts in precipitation intensity and runoff generation, the watershed's sustainability is increasingly threatened, with significant implications for ecosystem health and regional development.

Previous research has highlighted the watershed's susceptibility to hydrological extremes, including floods and soil erosion, under evolving climatic conditions (Golshan et al., 2020; Dadashi et al., 2024). Given its hydrological significance and sensitivity to climatic variability, the Gharesou watershed serves as an ideal case study for assessing the localized impacts of global climate change. Therefore, the primary objective of this study is to evaluate the performance of CMIP6 climate models within the Gharesou River basin and to project future precipitation and temperature regimes under diverse climate scenarios. These findings are intended to provide a robust scientific foundation for water resource management and policy-making in the region.

2. Material and Methods

2.1. Description of the study area

The Gharesou watershed, covering an area of approximately 4,062 km², is situated within the Ardabil Plain in northwestern Iran. As a major tributary of the Aras River, the Gharesou River is the primary drainage system for a significant portion of the province, contributing substantial surface runoff to the Aras basin. The watershed is characterized by a climatic gradient ranging from semi-arid to cold-mountainous conditions, with mean annual precipitation varying between 260 mm and 470 mm, primarily influenced by local topography and elevation (Golshan et al., 2020).

The basin features a complex physiography, with an elevation range extending from approximately 1,290 m to over 4,780 m above sea level. This substantial relief makes the watershed highly sensitive to shifts in precipitation regimes, thermal fluctuations, and snow dynamics, including snow accumulation and melt processes (Hazbavi et al., 2025). Seasonally, the watershed experiences peak precipitation during the spring, while summer months typically exhibit the lowest rainfall (Naserabadi et al., 2014). To evaluate the spatio-temporal trends in precipitation, maximum temperature, and minimum temperature, historical daily data were obtained from four representative meteorological stations: Ardabil, Ardabil Airport, Namin, and Nir. These stations were selected based on the availability and reliability of their long-term historical records. The geographic distribution of these stations within the Gharesou watershed and Ardabil Province is illustrated in Figure 1.

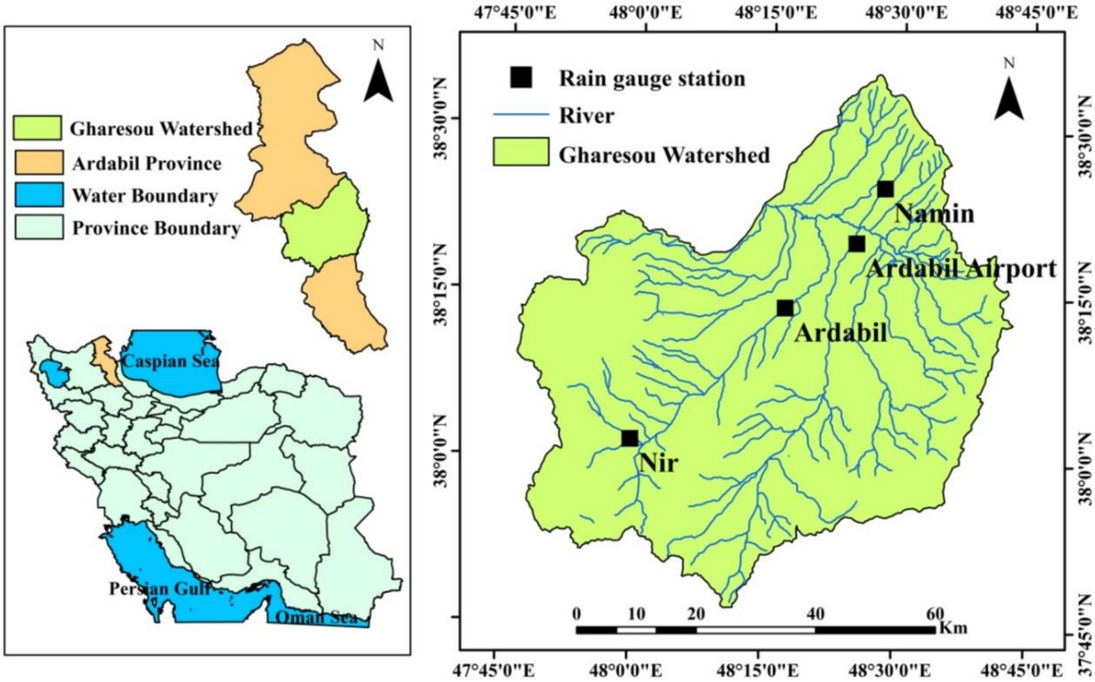

Figure 1. Location of the Gharesou watershed and the studied rain gauge stations in Ardabil Province

2.2. Research methodology

2.2.1. Global Climate Prediction Models

The CMIP6 framework encompasses a diverse suite of 55 climate models (Meresa et al., 2022). While these models provide critical insights into global climatic processes, they often exhibit inherent biases when simulating regional historical climate data and future projections. The objective of this study is to project daily precipitation, maximum temperature T_{max}, and T_{min} temperature under three Shared Socioeconomic Pathways (SSPs): SSP1-2.6 (optimistic), SSP2-4.5 (intermediate), and SSP3-7.0 (pessimistic).

The selection of specific models for this study was guided by a multi-criteria approach. First, we prioritized models previously validated and demonstrated to perform well within the Iranian climate context, drawing upon the findings of Zarrin and Dadashi-Roudbari (2021), Ansari et al. (2022), and Zareian et al. (2023). Second, we mandated the availability of comprehensive daily historical data to facilitate rigorous model performance evaluation. A significant challenge in this selection process was the lack of temporal continuity in many models, as some failed to provide daily historical records or simultaneous projections for the required variables P, T_{max}, and T_{min} across all three targeted SSP scenarios. By screening the CMIP6 archive against these stringent data-availability and regional-suitability criteria, three models were selected for this study. The specifications of these selected climate models are detailed in Table 1.

Table 1. General information on the selected CMIP6 models (adapted from https://pcmdi.llnl.gov/index.html)

Climate Model	Country	Organization	Spatial Resolution
ACCESS-CM2	Australia	Commonwealth Scientific and Industrial Research Organisation (CSIRO)	250 km
MIROC6	Japan	Japan Agency for Marine-Earth Science and Technology (JAMSTEC), Atmosphere and Ocean Research Institute, National Institute for Environmental Studies, and RIKEN Center for Computational Science (MIROC)	250 km
NESM3	China	Nanjing University of Information Science and Technology (NUIST)	2.5 degree

2.2.2. Selection of appropriate climate models based on evaluation criteria

To use future projections from global climate models, it is essential to evaluate their historical data against observed data from the study stations. Accordingly, historical data from three models (ACCESS-CM2, MIROC6, and NESM3) for daily precipitation, maximum temperature, and minimum temperature were obtained from https://cds.climate.copernicus.eu/cdsapp#!/dataset/projections-cmip6?tab=form for the period 1984 to 2014 (according to the release date of CMIP6, historical data are available up to 2014). The study stations' observational data quality was assessed, focusing on missing or incorrect entries. The evaluation of historical data provided by the global climate models was conducted using the Percent Bias (PBIAS), Root Mean Squared Error (RMSE), and Nash-Sutcliffe Efficiency (NSE) criteria.

The PBIAS index (Equation 1) measures the average tendency of simulated values to be larger or smaller than observed values. A value of zero indicates perfect agreement, positive values indicate underestimation, and negative values indicate overestimation (Moriasi et al., 2007). The RMSE index (Equation 2) calculates the root mean square error between observed and simulated values; a value of zero indicates perfect agreement (Dawson et al., 2007). The NSE index (Equation 3), which indicates the agreement between observed and simulated values, ranges from −∞ to 1. A value of 1 indicates perfect agreement, while values less than zero indicate unacceptable model performance (Moriasi et al., 2007).

$$PBIAS = 100 \times \left[\frac{\sum_{i=1}^{n}(y_{obs} - y_{sim})}{\sum_{i=1}^{n}(y_{obs})}\right] \quad (1)$$

$$RMSE = \sqrt{\frac{1}{n}\sum_{i=1}^{n}|y_{obs} - y_{sim}|^2} \quad (2)$$

$$NSE = 1 - \frac{\sum_{i=1}^{n}(y_{sim} - y_{obs})^2}{\sum_{i=1}^{n}(y_{obs} - \overline{y_{obs}})^2} \quad (3)$$

Where y_{obs} is the observed value of the variable, y_{sim} is the predicted value of the variable, and $\bar{y}_{obs}$ is the mean of the observed values.

2.2.3. Future climate projection data used

Although CMIP6 models capture global-scale climate evolution, their raw outputs typically require downscaling and bias correction to be applicable at the local scale. In this study, future daily precipitation, T_{max}, and T_{min} for the period 2025–2054 were generated by applying the Change Factor (CF) method—also referred to as the Delta Change Method—to correct biases in the large-scale climate model outputs relative to historical observations (Khordadi et al., 2014; Wu et al., 2023).

The CF method is a widely utilized approach in hydrological and climate impact assessments due to its ability to incorporate projected climate signals into historical observational records, thereby preserving

local climatic characteristics (Hay et al., 2000; Fowler et al., 2007). The primary advantages of this method include its computational efficiency, transparency, and minimal requirement for complex calibration. By utilizing observed records as a baseline, the method effectively preserves site-specific variability and mitigates systematic biases inherent in raw climate model outputs (Fowler et al., 2007; Anandhi et al., 2011). While it is acknowledged that the CF approach primarily adjusts the mean and may overlook changes in distributional extremes (Teutschbein & Seibert, 2012), it remains a robust and highly accepted technique for transferring climate change signals from GCMs to local-scale observations (Hay et al., 2000; Fowler et al., 2007). To implement this method, monthly mean values were calculated for both the historical (1984–2014) and future (2025–2054) periods. The climate change signals were subsequently derived using the following formulations (Wu et al., 2023):
For precipitation, the ratio of future-to-historical monthly mean values was calculated (Equation 4).

$$\Delta P_i = (P_{GCM,FUT,i}/P_{GCM,base,i}) \quad (4)$$

$$\Delta T_i = (\bar{T}_{GCM,FUT,i} - \bar{T}_{GCM,base,i}) \quad (5)$$

Where, ΔP_i and ΔT_i are the precipitation and temperature change scenarios for a long-term monthly mean for each month (i=1, ..., 12); $P_{GCM,FUT,i}$ is the long-term monthly mean precipitation simulated by the model for the future period; $P_{GCM,base,i}$ is the long-term monthly mean precipitation simulated by the model for the historical period; $\bar{T}_{GCM,FUT,i}$ is the long-term monthly mean temperature simulated by the model for the future period; and $\bar{T}_{GCM,base,i}$ is the long-term monthly mean temperature simulated by the model for the historical period (Anandhi et al., 2011; Wu et al., 2023). Subsequently, the time series of future climate scenarios were obtained using Equations 6 and 7:

$$P = (P_{obs} \times \Delta P) \quad (6)$$

$$T = (T_{obs} + \Delta T) \quad (7)$$

where P is the time series of future precipitation climate scenarios; P_{obs} is the time series of observed daily precipitation during the base period; ΔP is the downscaled precipitation climate scenarios; T is the time series of future temperature climate scenarios; T_{obs} is the time series of observed daily temperature during the base period; and ΔT is the downscaled temperature climate scenarios (Anandhi et al., 2011; Azari et al., 2017). For this study, future daily precipitation, T_{max}, and T_{min} projections for the 2025–2054 period were retrieved from the Coupled Model Intercomparison Project Phase 6 (CMIP6) data archive (https://cds.climate.copernicus.eu/) under the SSP1-2.6, SSP2-4.5, and SSP3-7.0 scenarios.

3. Results and Discussion

To determine the most suitable climate model for projecting future conditions, the historical outputs (1984–2014) of the candidate models were validated against observed meteorological records from the Ardabil, Ardabil Airport, Namin, and Nir stations, using the aforementioned statistical criteria. The performance of these models in simulating annual total precipitation and annual mean T_{max} and T_{min} is summarized in Tables 2 and 3, respectively.

Table 2. Evaluation results of historical daily precipitation data (annual total) of the selected models against observational data of the studied stations

Station	Climate Model	PBIAS	RMSE	NSE
Ardabil	ACCESS-CM2	54.60	205.36	-12.93
	MIROC6	83.80	254.26	-20.36
	NESM3	51.70	171.79	-8.75
Ardabil Airport	ACCESS-CM2	67.50	155.06	-36.35
	MIROC6	150.70	357.92	-198.00
	NESM3	88.20	208.59	-66.59
Namin	ACCESS-CM2	51.90	145.33	-18.18
	MIROC6	113.70	342.19	-105.36
	NESM3	63.50	187.33	-30.88
Nir	ACCESS-CM2	16.90	102.88	-2.14
	MIROC6	65.90	306.21	-26.84
	NESM3	27.40	154.01	-6.04

Table 3. Evaluation results of historical daily maximum and minimum temperature data (annual mean) of the selected models against observational data of the studied stations

Station	Climate Model	Max Temp PBIAS	Max Temp RMSE	Max Temp NSE	Min Temp PBIAS	Min Temp RMSE	Min Temp NSE
Ardabil	ACCESS-CM2	-22.70	4.34	-9.98	20.10	2.02	-2.95
	MIROC6	61.80	9.82	-55.22	261.50	8.14	-62.97
	NESM3	-24.10	4.89	-12.93	225.90	7.42	-52.19
Ardabil Airport	ACCESS-CM2	-28.40	4.68	-22.13	59.70	1.45	-7.06
	MIROC6	57.40	9.33	-90.77	443.20	9.34	-331.03
	NESM3	-29.70	4.97	-25.06	359.40	7.62	-220.16
Namin	ACCESS-CM2	-22.00	3.48	-9.27	-34.00	2.07	-8.36
	MIROC6	71.20	10.66	-95.32	112.90	6.19	-82.71
	NESM3	-20.70	3.37	-8.63	86.00	4.81	-49.57
Nir	ACCESS-CM2	-27.90	4.70	-14.03	3.20	1.10	-1.30
	MIROC6	57.00	9.34	-58.28	223.60	8.03	-121.05
	NESM3	-29.00	4.84	-14.93	175.30	6.30	-74.04

Table 2 evaluates three CMIP6 models (ACCESS-CM2, MIROC6, and NESM3) against observed annual precipitation at four stations. All models show positive PBIAS values, meaning they systematically overestimate precipitation. The NSE is negative for every model station combination, indicating that the models perform worse than simply using the observed mean. At Ardabil Airport, MIROC6 exhibits an extreme overestimation (PBIAS=150.70) and an extremely poor NSE (-198.00), accompanied by a very high RMSE (357.92 mm). In contrast, ACCESS-CM2 model at Nir station shows the smallest bias (PBIAS=16.90) and the closest to zero NSE (-2.14), together with the lowest RMSE (102.88 mm). Overall, the ACCESS-CM2 model has the lowest PBIAS, NSE, and RMSE values at Ardabil Airport, Namin, and Nir stations compared to other models. At Ardabil station, the lowest PBIAS, NSE, and RMSE values is related to the NESM3 model.

Table 3 summarises the performance of the same models for annual mean maximum and minimum temperature. For maximum temperature, ACCESS-CM2 and NESM3 models show negative PBIAS (underestimation), whereas MIROC6 shows strong positive bias (overestimation). For minimum temperature, nearly all PBIAS values are positive and extremely large, indicating a dramatic overestimation of minimum temperatures. The largest discrepancies are observed for maximum temperature with MIROC6 at Namin station (PBIAS=71.20, NES=-95.32, and RMSE=10.66 °C), and for minimum temperature with MIROC6 at Ardabil

Airport station (PBIAS=443.20, NES=-331.03, and RMSE=9.34 °C). In contrast, for maximum temperature NESM3model at Namin station shows the smallest bias (PBIAS=-20.70) and the closest to zero NSE (-8.63), together with the lowest RMSE (3.37 °C). For minimum temperature ACCESS-CM2 model performs best at Nir station with PBIAS=3.20, NSE=-1.30, and RMSE=1.10 °C. Overall, the ACCESS-CM2 model has the lowest PBIAS, NSE, and RMSE rates for maximum and minimum temperatures at all stations except for the maximum temperatures at the Namin station.

It is widely recognized that GCM outputs often lack the necessary precision for local-scale applications due to their coarse spatial resolution and inherent systematic biases (Teutschbein & Seibert, 2012). Consequently, climate impact assessments typically employ performance metrics to rank candidate models, despite the persistent uncertainties and errors associated with simulating regional climate conditions. To mitigate these discrepancies, bias-correction and downscaling techniques are essential prerequisites for generating reliable future projections (Ashfaq et al., 2022; Azad & Ahmadi, 2024). In the current study, the ACCESS-CM2 model was prioritized based on its superior performance across all meteorological stations, consistently demonstrating lower RMSE and PBIAS, alongside higher NSE values compared to the MIROC6 and NESM3 models.

To project future climatic conditions (2025–2054), daily precipitation, T_{max}, and T_{min} data were bias-corrected using the Change Factor (CF) method applied to the ACCESS-CM2 outputs under the SSP1-2.6, SSP2-4.5, and SSP3-7.0 scenarios. The projected mean monthly and annual precipitation trends for the Ardabil, Ardabil Airport, Namin, and Nir stations are illustrated in Figures 2 and 3.

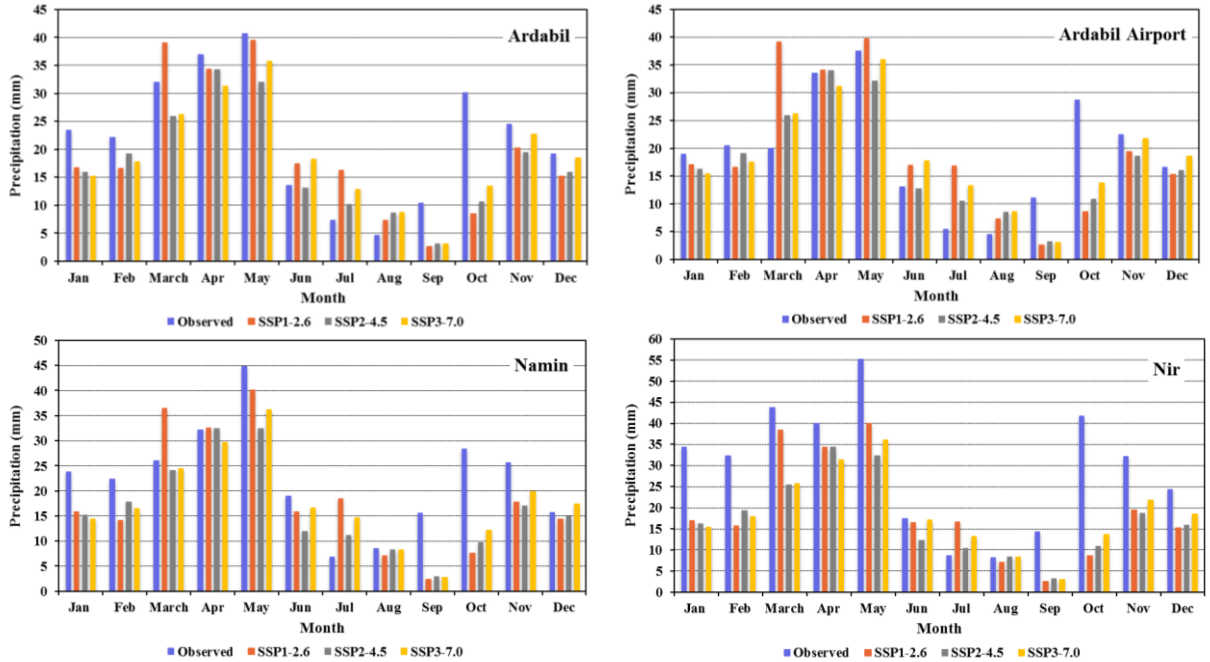

Figure 2. Observed and future projected mean monthly precipitation (mm) under three climate scenarios at the study stations of the Gharesou watershed

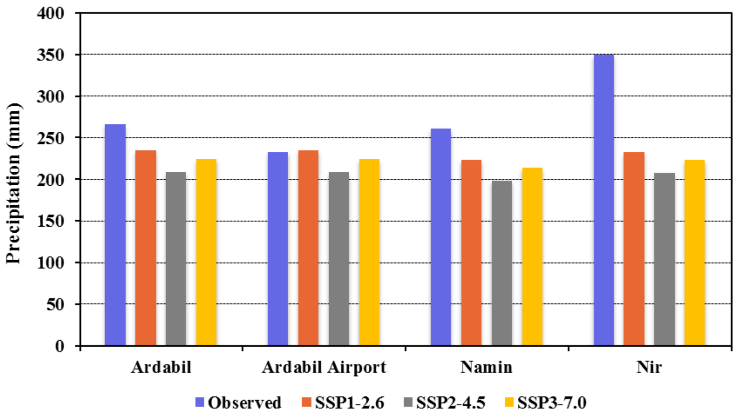

Figure 3. Observed and future projected mean annual precipitation (mm) under three climate scenarios at the study stations of the Gharesou watershed

As illustrated in Figure 2, the seasonal distribution of both observed and projected precipitation indicates a peak during the spring months (March–May), with the lowest values occurring during the summer (July–September). The projections reveal a generalized downward trend in monthly precipitation across all scenarios compared to the historical baseline, with specific exceptions: June–August in Ardabil; March and June–August at the Ardabil Airport; and July at the Namin and Nir stations. This trend of decreasing precipitation aligns with findings reported by Zarrin and Dadashi-Roudbari (2021), Wang et al. (2023), and Wu et al. (2023). The most substantial discrepancies between historical and projected values are observed in September and October across all study stations. This deviation may be attributed to the cold-climate characteristics of the region, where the onset of autumn precipitation may not be fully captured by the selected climate model. Notably, the Nir station exhibits the highest monthly precipitation, reaching a historical peak of 55 mm in May, where the variance between observed and projected values is particularly pronounced throughout most of the year.

Annual precipitation trends presented in Figure 3 confirm a consistent decline under all three future scenarios at all stations, a result consistent with the observations of Ansari et al. (2022) regarding precipitation trends in western Iran. Under the SSP1-2.6 scenario, the mean annual precipitation is projected to decrease by 31.07 mm, 37.60 mm, and 116.69 mm at the Ardabil, Namin, and Nir stations, respectively, while a marginal increase of 1.44 mm is projected for the Ardabil Airport station. Under the SSP2-4.5 scenario, reductions of 57.01 mm, 24.66 mm, 62.57 mm, and 141.22 mm are projected for the Ardabil, Ardabil Airport, Namin, and Nir stations, respectively. For the SSP3-7.0 scenario, the corresponding decreases are 41.22 mm, 8.91 mm, 47.20 mm, and 125.79 mm. It is noteworthy that the projected reduction in precipitation is most pronounced under the SSP2-4.5 (intermediate) scenario, exceeding the declines observed in both the optimistic (SSP1-2.6) and pessimistic (SSP3-7.0) scenarios. Finally, Figures 4 and 5 illustrate the observed and projected mean monthly and annual T_{max} values, respectively, for the stations within the Gharesou watershed

.

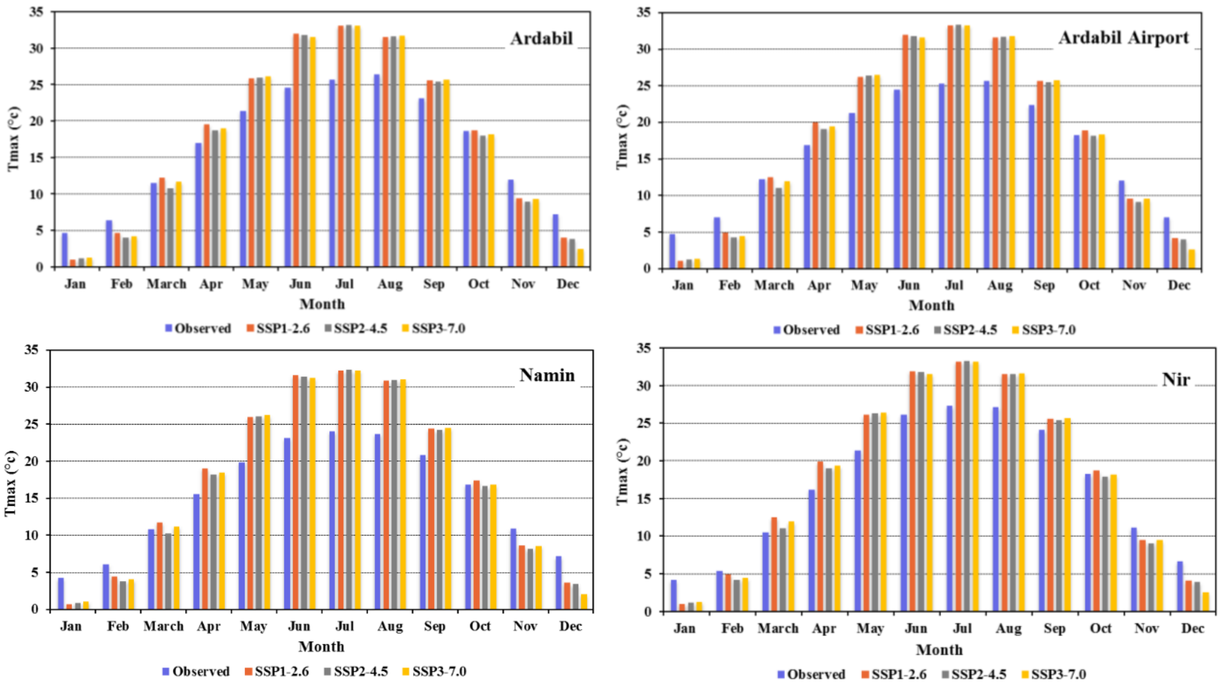

Figure 4. Observed and future projected mean monthly maximum temperature (°C) under three climate scenarios at the study stations of the Gharesou watershed

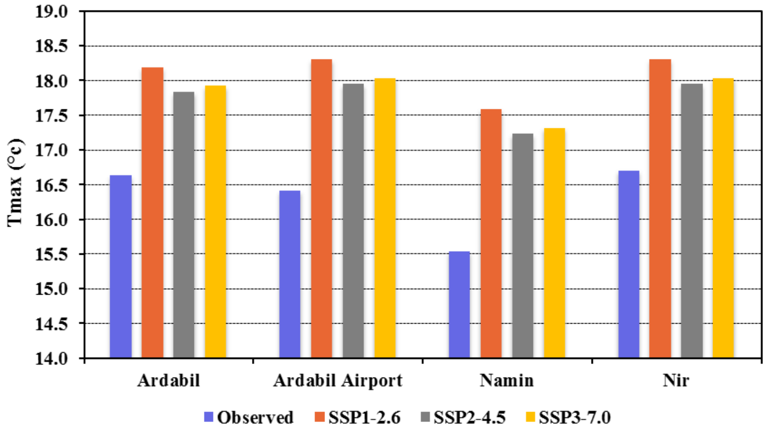

Figure 5. Observed and future projected mean annual maximum temperature (°C) under three climate scenarios at the study stations of the Gharesou watershed

Analysis of mean monthly maximum temperatures (Figure 4) indicates a general increase in projected future temperatures compared to the historical baseline, with the exception of the winter and late-autumn months (January–March and November–December). Peak maximum temperatures are projected to occur during the summer (June–August), with observed increases ranging from approximately 4.36 °C (SSP1-2.6, Nir, August) to 8.52 °C (SSP1-2.6, Namin, June). Conversely, projected decreases during the winter months vary between 1.61 °C (SSP1-2.6, Nir, November) and 5.07 °C (SSP3-7.0, Namin, December). Similar fluctuations in temperature trends—exhibiting both increases and decreases relative to historical records—have been documented by Ansari et al. (2022).

As presented in Figure 5, all future climate scenarios project a consistent rise in annual maximum temperatures across the study area, a finding supported by previous regional assessments in Iran (Iranshahi et al., 2023; Ansari et al., 2022). Interestingly, the results suggest that the SSP1-2.6 (optimistic) scenario projects a greater increase in maximum temperatures compared to the intermediate and pessimistic scenarios. Although higher-emission pathways are theoretically expected to drive more severe warming globally, regional projections often deviate from this hierarchy. This behavior is attributed to the influence of internal climate variability, regional atmospheric circulation patterns, and land–atmosphere feedbacks, which can exert a more pronounced influence than greenhouse gas forcing at the watershed scale. Furthermore, model-related uncertainties and the dominance of natural variability in the near-future period (2025–2054) may cause lower-emission scenarios to show higher temperature shifts than high-emission scenarios. Consequently, such inconsistencies in scenario ordering should be interpreted as manifestations of regional climatic complexity and model uncertainty rather than a contradiction of the fundamental climate change signal (Hawkins and Sutton, 2009; IPCC, 2021).

Figures 6 and 7 illustrate the observed and projected mean monthly and annual minimum temperatures (T_{min}) under the three SSP scenarios across all study stations in the Gharesou watershed."

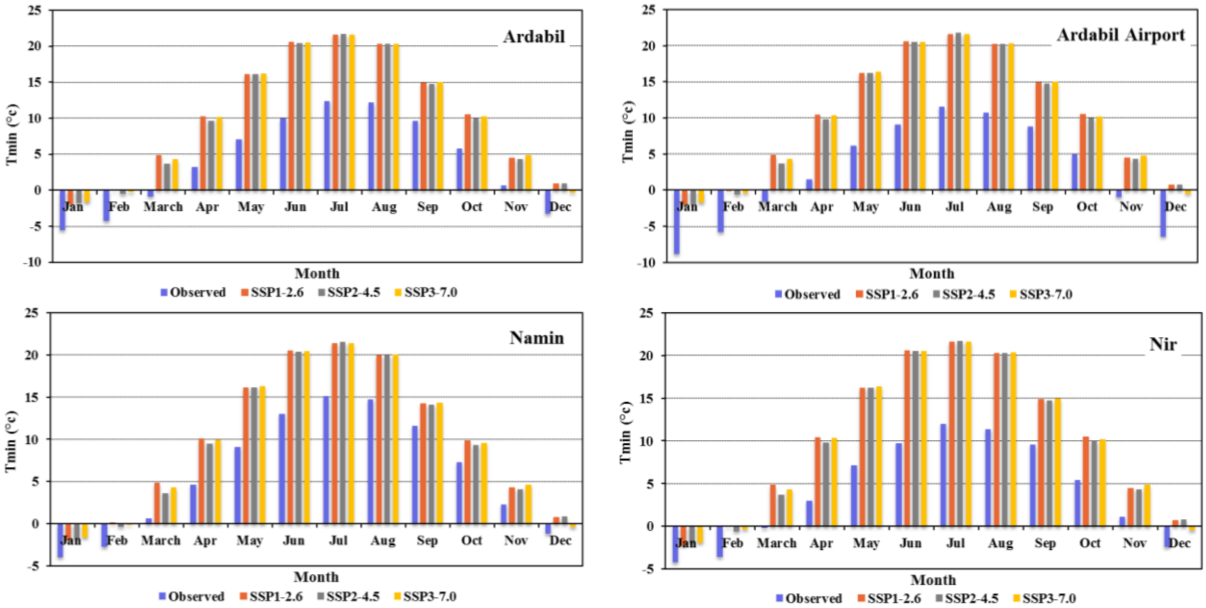

Figure 6. Observed and future projected mean monthly minimum temperature (°C) under three climate scenarios at the study stations of the Gharesou watershed

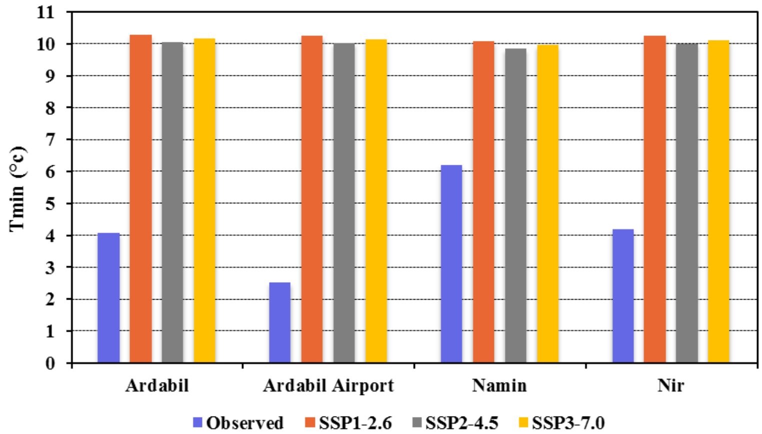

Figure 7. Observed and future projected mean annual minimum temperature (°C) under three climate scenarios at the study stations of the Gharesou watershed

minimum temperatures typically occur during the winter months (December–February). The projections for mean

As shown in Figure 6, the lowest monthly minimum temperatures reveal a consistent increasing trend throughout the year across all study stations compared to the historical baseline. This warming signal ranges from a minimum of 0.77 °C (December, Namin station, SSP3-7.0) to a maximum of 11.5 °C (June, Ardabil Airport station, SSP1-2.6). Furthermore, Figure 7 illustrates a significant rise in annual minimum temperatures, with projections ranging from an increase of 3.65 °C (Namin, SSP2-4.5) to 7.75 °C (Ardabil Airport, SSP1-2.6).

It is essential to recognize that historical model biases do not necessarily dictate the direction or magnitude of future projections. Climate change assessments primarily rely on the climate change signals generated by GCMs rather than their absolute values during the baseline period. Consequently, a model may exhibit a systematic underestimation of observed temperatures (PBIAS < 0) while simultaneously projecting a robust warming trend under future emission scenarios. This phenomenon is a well-documented aspect of climate modeling, emphasizing the critical distinction between inherent model bias and the projected climatic response to anthropogenic greenhouse gas forcing (Teutschbein and Seibert, 2012; IPCC, 2021).

4. Conclusion

Climate change represents one of the most critical environmental challenges of the 21st century, with profound implications for natural resources, agriculture, and socio-economic stability. Given the recent increase in extreme hydro-climatic events—such as floods and droughts—that have caused significant infrastructural and economic damage in Iran, this study aimed to project future precipitation and temperature regimes in the Gharesou watershed. By evaluating CMIP6 models, we identified ACCESS-CM2 as the most suitable model for this region, outperforming others in simulating historical precipitation and minimum temperature.

Our projections for the 2025–2054 period reveal a distinct transition toward warmer and drier climatic conditions in the Gharesou watershed. The results consistently indicate a reduction in annual precipitation across all studied stations, with the most pronounced decreases observed under the intermediate SSP2-4.5 scenario. Concurrently, both maximum and minimum temperatures are expected to rise significantly, with summer monthly maximum temperatures projected to increase by over 5 °C at several locations. These findings underscore a regional shift from a cold-mountainous climate toward more arid and thermal conditions.

While these projections provide a vital evidence base, it is important to acknowledge inherent uncertainties stemming from inter-model differences, emission scenario assumptions, and the limitations of the Change Factor method in capturing shifts in climatic variability and extreme events (IPCC, 2023; Maraun, 2016). Nevertheless, the alignment of our projected trends with observed historical data and recent regional studies (e.g., Esgandari et al., 2024; Gimechi et al., 2025) reinforces the reliability of our findings. The combination of decreasing precipitation and rising temperatures is expected to exacerbate challenges related to water scarcity, reduced groundwater recharge, and increased evapotranspiration, thereby threatening agricultural productivity and food security.

Ultimately, these results serve as a compelling call for proactive, science-based water resource management in the Gharesou watershed. Given the watershed's role as a vital agricultural and environmental hub, stakeholders must integrate these climate projections into long-term planning. Strengthening resilience against hydrological extremes, promoting sustainable land-use practices, and improving water-use efficiency are essential steps for mitigating the adverse impacts of a changing climate and ensuring regional sustainable development.

Declarations

Conflict of interests

The authors declare that they have no competing or conflict of interests.

Data Availability Statement

All data generated or analyzed during this study are included in this published article.

Acknowledgement

This work is based upon research funded by Iran National Science Foundation (INSF) under project No.4037755

Authors' contributions

All authors contributed to the study conception and design. Material preparation, data collection and analysis were performed by authors. All authors read and approved the final manuscript.

References

[1]. Alimohamadian, L., Mostafazadeh, R., & Mirzaei Hassanlu, A. (2026). Estimating the variability of climate temperature extremes using statistical distributions over a diverse climatic region. *Geomatics, Natural Hazards and Risk*, *17*(1), 2608251.

[2]. Anandhi, A., Frei, A., Pierson, D. C., Schneiderman, E. M., Zion, M. S., Lounsbury, D., & Matonse, A. H. (2011). Examination of change factor methodologies for climate change impact assessment. *Water Resources Research*, *47*(3).

[3]. Ansari, S., Dehban, H., Zareian, M., & Farokhnia, A. (2022). Investigation of temperature and precipitation changes in the Iran's basins in the next 20 years based on the output of CMIP6 model. *Iranian Water Research Journal*, *16*(1), 11-24.

[4]. Asgari, E., Mostafazadeh, R., & Talebi Khiavi, H. (2025). Projecting the climate change impact on water yield in a cold mountainous watershed, ardabil. *Journal of the Earth and Space Physics*, *50*(4), 165-177.

[5]. Ashfaq, M., Rastogi, D., Kitson, J., Abid, M. A., & Kao, S. C. (2022). Evaluation of CMIP6 GCMs over the CONUS for downscaling studies. Journal of Geophysical Research: Atmospheres, 127(21), e2022JD036659.

[6]. Azad, N., & Ahmadi, A. (2024). Assessment of CMIP6 models and multi-model averaging for temperature and precipitation over Iran. Scientific Reports, 14(1), 24165.

[7]. Azari, M., Saghafian, B., Moradi, H. R., & Faramarzi, M. (2017). Effectiveness of soil and water conservation practices under climate change in the Gorganroud Basin, Iran. *CLEAN–Soil, Air, Water*, *45*(8), 1700288.

[8]. Coelho, G. D. A., Ferreira, C. M., Johnston, J., Kinter III, J. L., Dollan, I. J., & Maggioni, V. (2022). Potential impacts of future extreme precipitation changes on flood engineering design across the contiguous United States. *Water Resources Research*, *58*(4), e2021WR031432.

[9]. Dadashi, R., Esmali-Ouri, A., Mostafazadeh, R., & Haji, K. (2024). Multi-criteria evaluation of the environmental carrying capacity (ECC) of Gharesou watershed in Ardabil province to optimal utilization of watershed resource. *Environmental Earth Sciences*, *83*(4), 131.

[10]. Dannenberg, M. P., Wise, E. K., & Smith, W. K. (2019). Reduced tree growth in the semiarid United States due to asymmetric responses to intensifying precipitation extremes. *Science advances*, *5*(10), eaaw0667.

[11]. Dawson, C. W., Abrahart, R. J., & See, L. M. (2007). HydroTest: a web-based toolbox of evaluation metrics for the standardised assessment of hydrological forecasts. *Environmental Modelling & Software*, *22*(7), 1034-1052.

[12]. Döscher, R., Acosta, M., Alessandri, A., Anthoni, P., Arneth, A., Arsouze, T., ... & Zhang, Q. (2021). The EC-earth3 Earth system model for the climate model intercomparison project 6. *Geoscientific Model Development Discussions*, *2021*, 1-90.

[13]. Esgandari, R., Esmali Ouri, A., Mostafazadeh, R., & Choobeh, S. (2024). Assessment of temporal and spatial variations of precipition climate extreme indexes in the central part of Ardabil

province. Journal of Environmental Science Studies, 9(1), 8119-8133.

[14]. Estoque, R. C., Ooba, M., Togawa, T., & Hijioka, Y. (2020). Projected land-use changes in the Shared Socioeconomic Pathways: Insights and implications. *Ambio*, *49*(12), 1972-1981.

[15]. Eyring, V., Bony, S., Meehl, G. A., Senior, C. A., Stevens, B., Stouffer, R. J., & Taylor, K. E. (2016). Overview of the Coupled Model Intercomparison Project Phase 6 (CMIP6) experimental design and organization. *Geoscientific Model Development*, *9*(5), 1937-1958.

[16]. Fowler, H. J., Blenkinsop, S., & Tebaldi, C. (2007). Linking climate change modelling to impacts studies: recent advances in downscaling techniques for hydrological modelling. *International Journal of Climatology: A Journal of the Royal Meteorological Society*, *27*(12), 1547-1578.

[17]. Gimechi, S., Mostafazadeh, R., & Alimohamadian, L. (2025). Analysis of extreme precipitation trends and probability distributions across return periods in northwest Iran. Geografický časopis/Geographical Journal, 77(1), 43-55.

[18]. Golshan, M., Kavian, A., Esmali, A., & Ziegler, A. D. (2020). Runoff and sediment yield modeling in data-sparse catchments in the Garehsoo River basin, northern Iran. *Environmental Earth Sciences*, *79*(14), 351.

[19]. Hawkins, E., & Sutton, R. (2009). The potential to narrow uncertainty in regional climate predictions. *Bulletin of the American Meteorological Society*, *90*(8), 1095-1108.

[20]. Hay, L. E., Wilby, R. L., & Leavesley, G. H. (2000). A comparison of delta change and downscaled GCM scenarios for three mountainous basins in the United States 1. *JAWRA Journal of the American Water Resources Association*, *36*(2), 387-397.

[21]. Hazbavi, Z., Azizi, E., Ghabelnezam, E., Sharifi, Z., Davudirad, A., & Fathololoumi, S. (2025). Enhancing Watershed Management Through the Characterization of the River Restoration Index (RRI): A Case Study of the Samian Watershed, Ardabil Province, Iran. *Earth*, *6*(1), 6.

[22]. Hussain, S., Mubeen, M., Nasim, W., Mumtaz, F., Abdo, H. G., Mostafazadeh, R., & Fahad, S. (2024). Assessment of future prediction of urban growth and climate change in district Multan, Pakistan using CA-Markov method. *Urban Climate*, *53*, 101766.

[23]. Intergovernmental Panel on Climate Change (IPCC). (2013). Climate Change 2013 - The Physical Science Basis. Working Group I Contribution to the Fifth Assessment Report of the Intergovernmental Panel on Climate Change. 1552p.

[24]. Intergovernmental Panel on Climate Change (IPCC). (2021). Climate Change 2021: The physical science basis. Contribution of Working Group I to the Sixth Assessment Report of the Intergovernmental Panel on Climate Change; technical summary.

[25]. Intergovernmental Panel on Climate Change (IPCC). (2023). Climate Change 2021 – The Physical Science Basis: Working Group I Contribution to the Sixth Assessment Report of the Intergovernmental Panel on Climate Change. Cambridge: Cambridge University Press.

[26]. Iranshahi, M., Ebrahimi, B., Yousefi, H., & Moridi, A. (2023). Investigating the effects of climate change on temperature and precipitation using neural network and CMIP6 (Case study: Aleshtar and Khorramabad Stations). *Water and Irrigation Management*, *12*(4), 821-845.

[27]. Khansalari, S., & Mohammadi, A. (2024). Probabilistic projection of extreme precipitation changes over Iran by the CMIP6 multi-model ensemble. *Climatic Change*, *177*(7), 115.

[28]. Khordadi, M. J., Alizadeh, A., Nassiri Mahallati, M., & Hooshmand, D. (2014). An evaluation of the impact of climate change on climatic parameters and dry and wet spells in the next 100 years using combining IDW and change factor methods (A case study in Tehran-Karaj

subbasin). *Journal of Geography and Regional Development*, *21*, 157-178.

[29]. Liu, J., Jiang, L., Zhang, X., Druce, D., Kittel, C. M., Tøttrup, C., & Bauer-Gottwein, P. (2021). Impacts of water resources management on land water storage in the North China Plain: Insights from multi-mission earth observations. *Journal of Hydrology*, *603*, 126933.

[30]. Luo, Q., & Yu, Q. (2012). Developing higher resolution climate change scenarios for agricultural risk assessment: progress, challenges and prospects. *International journal of biometeorology*, *56*(4), 557-568.

[31]. Maraun, D. (2016). Bias correcting climate change simulations-a critical review. *Current Climate Change Reports*, *2*(4), 211-220.

[32]. Meresa, H., Tischbein, B., & Mekonnen, T. (2022). Climate change impact on extreme precipitation and peak flood magnitude and frequency: observations from CMIP6 and hydrological models. *Natural Hazards*, *111*(3), 2649-2679.

[33]. Moriasi, D. N., Arnold, J. G., Van Liew, M. W., Bingner, R. L., Harmel, R. D., & Veith, T. L. (2007). Model evaluation guidelines for systematic quantification of accuracy in watershed simulations. *Transactions of the ASABE*, *50*(3), 885-900.

[34]. Mostafazadeh, R., Amini, H., & Adhami, M. (2025). Snow cover changes and affecting hydro-climate variables in Sabalan Mountainous region in Northwest Iran. Researches in Earth Sciences, 16(Special Issue), 18-30.

[35]. Naserabadi, F., Esmali Ouri, A., Akbari, H., & Rostamian, R. (2014). A sensitivity analysis of SWAT model in Ghareh Su watershed, Ardabil. *Watershed Engineering and Management*, *5*(4), 255-265.

[36]. Ouyang, F., Zhu, Y., Fu, G., Lü, H., Zhang, A., Yu, Z., & Chen, X. (2015). Impacts of climate change under CMIP5 RCP scenarios on streamflow in the Huangnizhuang catchment. *Stochastic environmental research and risk assessment*, *29*(7), 1781-1795.

[37]. Rogelj, J., Popp, A., Calvin, K. V., Luderer, G., Emmerling, J., Gernaat, D., ... & Tavoni, M. (2018). Scenarios towards limiting global mean temperature increase below 1.5 C. *Nature climate change*, *8*(4), 325-332.

[38]. Stocker, T.F., Qin, D., Plattner, G.K., Tignor, M., Allen, S.K., Boschung, J., Nauels, A., Xia, Y., Bex, V., and Midgley, P.M. (2013). Climate Change 2013, the Physical Science Basis. *Intergovernmental Panel on Climate Change*, 222p.

[39]. Su, B., Huang, J., Gemmer, M., Jian, D., Tao, H., Jiang, T., & Zhao, C. (2016). Statistical downscaling of CMIP5 multi-model ensemble for projected changes of climate in the Indus River Basin. *Atmospheric Research*, *178*, 138-149.

[40]. Teutschbein, C., & Seibert, J. (2012). Bias correction of regional climate model simulations for hydrological climate-change impact studies: Review and evaluation of different methods. *Journal of hydrology*, *456*, 12-29.

[41]. Voldoire, A., Saint-Martin, D., Sénési, S., Decharme, B., Alias, A., Chevallier, M., ... & Waldman, R. (2019). Evaluation of CMIP6 deck experiments with CNRM-CM6-1. *Journal of Advances in Modeling Earth Systems*, *11*(7), 2177-2213.

[42]. Wang, H., Jiang, P., Zhang, R., Zhao, J., Si, W., Fang, Y., & Zhang, N. (2023). The changing precipitation storm properties under future climate change. *Hydrology Research*, *54*(4), 580-590.

[43]. Wang, Q., Sun, Y., Guan, Q., Du, Q., Zhang, Z., Zhang, J., & Zhang, E. (2024). Exploring future trends of precipitation and runoff in arid regions under different scenarios based on a bias-corrected CMIP6 model. *Journal of Hydrology*, *630*, 130666.

[44]. Wu, Y., Ju, H., Qi, P., Li, Z., Zhang, G., & Sun, Y. (2023). Increasing flood risk under climate change and social development in the Second Songhua River

basin in Northeast China. *Journal of Hydrology: Regional Studies*, *48*, 101459.

[45]. Zareian, M. J., Dehban, H., & Gohari, A. (2023). Evaluation of the Accuracy of CMIP6 Models in Estimating the Temperature and Precipitation of Iran Based on a Network Analysis. *Water and Irrigation Management, 12 (4), 783-797*.

[46]. Zarrin, A., & Dadashi-Roudbari, A. (2021). Projection of future extreme precipitation in Iran based on CMIP6 multi-model ensemble: A. Zarrin, A. Dadashi-Roudbari. *Theoretical and Applied Climatology*, *144*(1), 643-660.